Design and Analysis of Frequency Switchable Dual Polarized Antenna for S-Band / WLAN Applications

Vinayagam K[1], SatheeshKumar Palanisamy[2,*] , Rajesh Natarajan[3], N. Sathishkumar[4], Aarthi Gunasekar[5]

[1] School of Electronics Engineering, Vellore Institute of Technology, Vellore, TamilNadu, 632014, India

E-mail: vinayagam.k2020@vitstudent.ac.in , Ph. :+918098830283

School of Electronics Engineering, Vellore Institute of Technology, Vellore – 632014, India , *E-mail: satheeshp@bmsit.in, Ph. :+91 9543234230*

[3]School of Electronics Engineering, Vellore Institute of Technology, Vellore, TamilNadu, 632014, India, E-mail: rajeshnatarajan44@gmail.com, Ph. :+91 9976254449

[4]Department of Electronics and Communication Engineering, KPR Institute of Engineering and Technology, Coimbatore - 641407 Tamil Nadu, India, E-mail: sathishkumar2490@gmail.com, Ph.:+91 9500595289

[5]School of Electronics Engineering, Vellore Institute of Technology, Vellore, TamilNadu, 632014, India, E-mail: aarthi.g@vit.ac.in, Ph.:+91 9003043086

*Corresponding Author

Abstract ─ This article provides the design of a dual frequency, dual-polarized microstrip patch antenna using a Single Rectangular Loop (SRL) element. The proposed antenna has a physical footprint of 50 x 40 x 1.2 mm^3 and a dielectric constant of 4.2. A single rectangular loop is placed with truncated corners on the inner patch to excite the right-hand circular polarization. The prototype is designed to operate in two modes with frequency and polarization re-configurability. The re-configurable mechanism is controlled by a pair of PIN diodes (BAR64-02V), which connect the inner patch and outer loop. In the ON state, the antenna exhibits right-hand circular polarization (RHCP) as a narrow-band antenna. It is capable of operating at frequencies between 5 GHz and 5.43 GHz. Furthermore, this device provides linear polarization (LP) in the frequency range of 3.75 GHz to 3.86 GHz. It exhibits 110 MHz of bandwidth in 3.8 GHz (S-band) and provides 430 MHz bandwidth in 5.2 GHz WLAN operating frequencies. The suggested antenna provides a maximum gain of 8.56 dBi. The antenna is fabricated and tested to prove its performance parameters. All the simulations are

performed using high Frequency Structure(HFSS) software and results are presented with discussions.

***Index Terms*—** Circular polarization, Reconfigurable antenna, PIN diode, Dual frequency antenna, Return loss.

I. INTRODUCTION

Nowadays, there has been much interest among researchers on multifunctional antennas. With the advent of an increasing population and the use of mobile phones, technology must cater to the needs of the users. Reconfigurable antennas are the suitable solution to the abovementioned problem. There are many ways to implement the reconfigurable antenna to serve for different applications. It is with respect to frequency, pattern, and polarization respectively. Out of which, polarization reconfigurability is taking much importance because it is the solution for interference suppression, overcoming multipath fading and increasing channel capacity. A low-profile Meta surface antenna is designed with square patch and pixel structure. Polarization and pattern diversity is induced with characteristic modes in [1]. Radiating patch and parasitic patches are connected with shorting pin to the ground which induced the wideband circular polarization through multimode resonance [2]. Microstrip patch with truncated corners excited via shared aperture induced polarization diversity in [3]. Four element antenna arrays with branch line coupler proposed for polarization diversity [4], where minimum PIN diodes are used for reconfiguration in millimetre waves. In [5], similar array system for polarization diversity is proposed with Substrate Integrated Waveguide(SIW) which is claimed for easy integration. Another wideband circular polarized antenna is designed with circular patches and metal rods connected to radiating patch provide AR bandwidth of 22.58% [6]. CP bandwidth is enhanced by inducing tri orthogonal modes with single feed in [7]. Polarization diverse antenna capable of changing between LP, LHCP and RHCP is proposed in [8] with arrow shaped driven element and quadruple gap coupled patches. An antenna that utilizes seven pin diodes and is corner truncated with polarization re-configurable in two switchable frequency bands is suggested [9]. In [10], circular loop loaded with four arc dipole and monopole is arranged with 12 pin diodes for exhibiting LP, HP and CP modes. Continuous polarization rotation is achieved with phase shifter network in [11] provide excellent cross polarization discrimination. A simple

antenna structure with 6 reconfigurable pattern and 3 polarization mode is achieved in [12]. Here, diagonal metallic walls with switches and pin diodes altered the current path on the radiating element provides multi polarized, multi directional antenna. Similar antenna is implemented with reflector plane in [13], achieved polarization diversity with high gain. Compact reconfigurable antenna is designed with reconfigurable feed network using phase shifters in [14-15] exhibits quad polarization diversity. Near field enabled parasitic Yagi driven antenna is proposed with directors and reflectors to provide quad polarization diversity in [16]. Fiber reinforced polymer composite cells are used a dielectric substrate for pattern and polarization diversity in [17], which avoids the use of semiconductor devices. Axial ratio improvement in array configuration [18], frequency and polarization switching via corner modification in [19] and [20] are with similar implementations. They designed a dual polarized antenna using varactors diode to achieved polarization reconfiguration [21]. The compact reconfigurable antenna is designed in[22], by using two ideal switches to perform Ultrawide Band(UWB) operation. They designed an antenna using radio frequency switches to be performed by frequency and pattern reconfigurable function [23]. In literature, most of the antenna layouts have large size, low bandwidth, low gain. The works have achieved dual function without circular polarization.

In this paper, dual frequency dual polarized antenna is designed with SRL element which operates in right-hand circular polarization (RHCP) and linear polarization (LP). The operating modes are obtained with the help of PIN diodes. This paper is arranged as follows. Section II described the design of the suggested dual frequency antenna with dimensional characteristics. Section III outlines the results and discussion. Conclusion and further scope on the antenna are incorporated in Section IV.

2. PROPOSED ANTENNA DESIGN

Though there are many implementations on dual frequency antenna, there are very few implementations available for dual polarized implementations. The design process of the suggested antenna is shown in Fig. 1. Table 1 summarizes the geometrical dimensions of proposed antenna

Fig. 1 A chart illustrating the antenna design process

Table 1. Geometrical dimensions of the proposed antenna (in mm)

The developed rectangular patch antenna infused with rectangular loop structure and the schematic is given in Fig. 2. The footprint of the antenna is 50 mm × 40 mm and fabricated on a FR-4 substrate. The design started with the rectangular patch of dimensions of 24 mm x 18 mm fed with coaxial cable with 50-ohm impedance matching. The antenna provides resonance at 5.2 GHz with linear polarization. To make this as a dual frequency implementation, a rectangular ring is embedded on the outer patch and the ring is connected to the patch via two PIN diodes. When the center patch is excited, the antenna provides resonance at 5.2 GHz which is due to the inner rectangular patch. When the diodes are ON, the entire radiating patch is considered as a single patch which exhibits resonance at 3.8 GHz.

The outer loop was designed to enhance the antenna's bandwidth and provide additional resonance modes. Its dimensions were carefully calculated from equations (1-4), to complement the central patch and optimize the overall frequency response. The loop creates a coupling effect with the central patch, which allows the antenna to operate at multiple frequencies or improve radiation characteristics such as gain and efficiency.

The feed position was chosen to ensure proper impedance matching and efficient power transfer between the transmission line and the antenna. By placing the feed at an optimal location, it was possible to minimize reflection and maximize radiation efficiency. The feed position was determined through simulation and experimental adjustments, ensuring that it achieves the desired resonance and polarization characteristics.

In order to select the antenna geometry, we use the following design equations (1–4).

To determine the rectangular patch width, we take into consideration

$$W = \frac{c}{2 f_0 \sqrt{\frac{2}{\varepsilon_r + 1}}} \qquad (1)$$

To determine the length of the rectangular patch,

$$L = L_{eff} - 2\Delta L \qquad (2)$$

Where

$$L_{eff} = \frac{c}{2 * f_r * \sqrt{\varepsilon_{r_{eff}}}} \quad (3)$$

c – velocity of light in air

f_r – resonant frequency

ε_r – relative dielectric constant (4.4)

The parameter ΔL is the extension of the length of the rectangular patch due to the fringing effects that occur at the edges of the patch. These fringing fields make the effective electrical length of the patch slightly longer than its physical length. To account for this, ΔL is added to both ends of the physical length of the patch to obtain the effective length.

For a breakdown of the formula for ΔL

$$\Delta L = 0.412h \frac{\left(\varepsilon_{r_{eff}} + 0.3\right)\left(\frac{W}{h} + 0.264\right)}{\left(\varepsilon_{r_{eff}} - 0.258\right)\left(\frac{W}{h} + 0.8\right)} \quad (4)$$

Where,

h - Substrate thickness or the height of the dielectric material

w - Width of the rectangular patch

$\varepsilon_r$eff - Effective dielectric constant

$$\varepsilon_{r_{eff}} = \frac{\varepsilon_r + 1}{2} + \frac{\varepsilon_r - 1}{2}\left(\frac{1}{\sqrt{1 + \frac{12h}{W}}}\right) \quad (5)$$

This equation (5) is derived experimentally, and ε_{reff} - generally lies between the dielectric constant of the substrate and that of air.

Fig.2. (a) Top view of the antenna geometry, (b) Bottom view of the antenna geometry in the schematic of the dual-mode antenna.

2.1. Working Principle of the Antenna

To excite circular polarization from the radiating patch, the corners are truncated to the inner rectangular patch. A small slit of 0.2 mm is implemented on diagonal edges with a distance of 1 mm from the corner. To excite orthogonal modes on the inner radiating patch, the coaxial feed is offset from the axis

center. The location of the slit decides the current rotation on circular path which contributes the right hand circular polarization. This is displayed in Figure 3. It is shown that the surface current is orthogonal on the corner of the radiating element which is highlighted with the arrowheads. The current is orthogonal between 0 degree and 180 degree and also between 270 degree and 360 degrees. To excite the second mode of operation, an outer ring is placed to enclose the inner patch. The distance between the patch and the ring is w4 = 1mm, to avoid mutual coupling. For a circular path of the electric field vector as an equation of space to exist, the electric field must consist of two orthogonal linear components that are identical in amplitude, and the phase distinction must be 90 degrees [24-25]. A horizontal plane E_H and a vertical plane E_V have identical amplitudes and are in phase quadrature ($\pm\pi/2$). It can be used to describe either RHCP or LHCP components in the equation(6).

$$E_{RHCP} = \frac{1}{\sqrt{2}}\left(E_H + jE_V\right)$$
$$E_{LHCP} = \frac{1}{\sqrt{2}}\left(E_H - jE_V\right) \quad (6)$$

The horizontal and vertical responses real and imaginary elements may be represented as (8):

$$E_H = E_A \operatorname{Cos}\left(H_P\right) + jH_A \operatorname{Sin}\left(H_P\right)$$
$$E_V = E_A \operatorname{Cos}\left(V_P\right) + jV_A \operatorname{Sin}\left(V_P\right) \quad (8)$$

The horizontal and vertical amplitudes (H_A, V_A), as well as the phase elements (H_P, V_P), are obtained at all directions in the antenna's far field [26-28].

[From this design consider all RHCP criteria is satisfied]

Fig.3. E field distribution of the designed antenna at 5.2 GHz (a) 0^0 (b) 180^0 (c) 270^0 (d) 360^0

Dual band functioning is illustrated in Figure 4 for various switching states in order to better understand how it works. With the help of the maximum current distribution[29], we determine the length of each slot contributing to each frequency band. According to the Fig. 4, state 1 is characterized by the highest current density at the center of the rectangular patch. Antennas operate at 3.5 GHz to cover the working frequency range. As a result of a change in the electrical length of a current distribution, frequency and polarization reconfiguration occurs in the antenna structure[30].

Single Rectangular Loop (SRL) antenna element is viable for the placement of the PIN diode (BAR64-02V)[31]. By activating or deactivating the outer rectangular patch, the electrical length of the proposed microstrip patch antenna can be adjusted. During forward bias, diode series inductance is L = 0.45 nH, while the resistance is R_s = 1.5 ohm. During reverse bias, the impedance is C_T = 0.25 pF. The circuit involves RF choke inductor and a DC blocking capacitor.

Fig. 4. RLC (lumped equivalent) model of PIN diodes (a) ON Condition (b) OFF Condition

The RF PIN diode is shown in Figure 4 as a lumped equivalent model (RLC)[32-33]. In the event that both diodes are ON, the antenna will act as narrow band with 3.8 GHz. When both diodes are OFF, the antennas working frequency changes from 3.8 GHz to 5.2 GHz due to the effect of rectangular ring resonators[34].

Fig. 5. Circuit diagram for DC biasing

Figure 5 shows a schematic representation of the DC biasing circuit[35]. An example of a simulation of a reflection coefficient plot at various states can be seen in figure 5. 5.2 GHz is achieved by the band stop filter by turning OFF diode D1 and D2 at the same time[36]. Since the rectangular ring resonators act as a band stop filter, the antenna operates at 3.8 GHz when diode D1 and D2 is ON.

3. RESULTS AND DISCUSSION

As part of the fabrication and testing process, the antenna is tested for its merits such as reflection coefficient and radiation characteristics. Field Fox network analyzer MS2027C VNA Master is used for reflection coefficient measurements[37-39]. A schematic of the antenna fabrication and measurement setup can be seen in Figure 6. Fabrication and testing of the suggested antenna are conducted in anechoic chambers[40]. This antenna is tested in the frequency range upto 6 GHz with an impedance of 50 Ω using the Amkom horn antenna as a reference antenna.

Fig.6. (a) VNA setup for antenna characterization, (b) Anechoic chamber setup, (c) Front view of the fabricated DRL antenna, (d) Back view of the fabricated DRL antenna.

In mode 1, the center patch is excited, and the diodes are OFF which gives resonance centered at 5.23 GHz with a bandwidth ranging from 5 GHz to 5.43 GHz. A comparison is made between the simulation and measurement results in Table 2. In the other mode, PIN diodes are placed between the patch and the rectangular ring. This increased the overall electrical dimension of the antenna. This gives resonance at 3.8 GHz with the bandwidth of 110 MHz at S band which is shown in Fig. 7. It gives additional ripples in the reflection characteristics due to the diode action, but this doesn't affect the resonance and the antenna bandwidth[41-42].

The evaluation steps of the proposed antenna and the reflection coefficient are depicted in Fig. 7(a). The proposed antenna is implemented with four steps. In step1, the rectangular patch antenna was designed for 5.2 GHz with coaxial feed which creates wide resonance and below -10 dB is observed. In step2, a slit is introduced on right side top corner of the rectangular patch which leads to poor impedance matching. Another slit is introduced on left side bottom corner of the rectangular patch, resonant frequency of 5.2 GHz is observed with less than -3 dB axial ratio in step 3[43-44]. Finally, in step 4, outer rectangular loop is introduced around patch, a best impedance matching is attained.

Fig . 7. S-Parameter (S_{11}) Characteristics of the Proposed Antenna
(a) Variations with respect to evolutionary Steps
(b) Variations with respect to Mode 1 and Mode 2

The proposed antenna works in the range of 5 GHz and 5.43 GHz. The absolute bandwidth is approximately 430 MHz, Peak return loss is -21 dB. Furthermore, this device provides linear polarization (LP) in the frequency range of 3.75 GHz to 3.86 GHz. The antenna exhibits 110 MHz of bandwidth in 3.8 GHz (S band) and peak return loss is -20 dB. The VSWR value falls within the range of 1 to 2 for the frequency range of 3 to 6 GHz.

3.1 Antenna Performance

Axial ratio bandwidth is playing an important role in circularly polarized antennas. The suggested antenna is developed to exhibit circular polarization in mode 1 where the inner patch alone get excited

with orthogonal modes [45]. To obtain CP, small slit of 0.2 mm is etched on the diagonal corners for the desirable operation of the antenna.

Fig. 8. Axial Ratio for Various Slot Widths (S_1 = 0.1 mm, 0.2 mm, and 0.3 mm)

The position of the slit determines the axial ratio bandwidth centered at 5 GHz which is experimented with different locations and different length. The frequency ranges from (4.92-5.23) GHz. The absolute bandwidth of 310 MHz is attained. The effect of various slot widths in axial ratio is shown in Fig. 8. It is referred from figure that the axial ratio is less than 3 dB for the slit of 0.2 mm. Fig. 9 shows the gain of the antenna in two radiating modes with the gain of 8.56 dBi and 5.96 dBi respectively.

Fig.9. Gain and Efficiency Parametric Analysis (Measured vs. Simulated)

The simulation and testing outcomes of the antenna are presented in Table 2. As a result, the measured and simulated outcomes are in agreement. A low-quality factor value for the diodes and losses in the biasing circuit cause the differences between the simulation and measurement results.

Table 2. Parametric Analysis of Antenna under Various Operating Conditions of Diode

Figure 10 illustrates the simulated and measured antenna radiation characteristics in both modes. The E plane shows the main beam is oriented along 0º for 5.2 GHz and 3.8 GHz which is evident from Figure. As expected, cross-polarization scores are significantly lower than co-polarization across all angles. This results in a directional radiation pattern that meets the required initial criteria.

Fig. 10. 2D Radiation Pattern for Observing the parametric Characteristics of the Antenna (a) 5.2 GHz (b) 3.8 GHz

In Table 3, the proposed work is compared with the existing work in terms of performance. We have considered similar frequency ranges for effective comparison. From the table, proposed antenna

exhibits two polarizations with high gain and impedance bandwidth compared with the work listed in the table.3.

Table 3. Comparative Analysis of the Proposed Antenna with a Relevant Antenna in Observing Parametric Characteristics

4. CONCLUSION

This paper presented the design of dual frequency dual polarized antenna using single rectangular loop for S band and WLAN communications. Single rectangular loop (SRL) element is proposed with full ground plane with coaxial feed. Small slits are imposed on the center rectangular patch to induce the orthogonal modes which gives circular polarization at 5.2 GHz. The re-configurable mechanism is controlled by a pair of PIN diodes which connect the inner patch and outer loop. In the ON state, the antenna exhibits right hand circular polarization (RHCP) as a narrow band antenna. It is capable of operating at frequencies between 5 GHz and 5.43 GHz. Furthermore, this device provides linear polarization (LP) in the frequency range of 3.75 GHz to 3.86 GHz. The antenna exhibits 110 MHz of bandwidth in 3.8 GHz (S band) and provides 430 MHz bandwidth in 5.2 GHz WLAN operating frequencies. The proposed antenna provides an average gain of 7 dBi. The antenna gives a reasonable AR bandwidth of 311 MHz. The rectangular loop embedded to the envelope of the rectangular patch excited and gives resonance at 3.8 GHz. The antenna provides reasonable gain of 8.56 dBi and 5.96 dBi, in respective modes. The effect of active elements on the antenna performance is negligible in this work.

REFERENCES

[1] Li W., Wang Y., M. M., Hei Y., et al. "A compact low-profile reconfigurable metasurface antenna with polarization and pattern diversities." *IEEE Antennas and Wireless Propagation Letters* 20.7 (2021): 1170-1174. https://doi.org/10.1109/lawp.2021.3074639.

[2] Hu W., Li C., Liu X., et al. "Wideband circularly polarized microstrip patch antenna with multimode resonance." *IEEE Antennas and Wireless Propagation Letters* 20.4 (2021): 533-537. https://doi.org/10.1109/lawp.2021.3056404.

[3] Wang S., Yang D., Geyi W., et al. "Polarization-reconfigurable antenna using combination of circular polarized modes." *IEEE Access* 9 (2021): 45622-45631. https://doi.org/10.1109/access.2021.3067064.

[4] Tsao Y.F., Desai A., Hsu H.T. "Dual-band and dual-polarization CPW-fed MIMO antenna for fifth-generation mobile communications technology at 28 and 38 GHz." *IEEE Access* 10 (2022): 46853-46863. https://doi.org/10.1109/access.2022.3171248.

[5] Cheng Y., Yang, Yuandan D. "Wideband circularly polarized planar antenna array for 5G millimeter-wave applications." *IEEE Transactions on Antennas and Propagation* 69.5 (2020): 2615-2627. https://doi.org/10.1109/tap.2020.3028213.

[6] Cheng Y., Yang, Yuandan D. "Wideband circularly polarized split patch antenna loaded with suspended rods." *IEEE Antennas and Wireless Propagation Letters* 20.2 (2020): 229-233. https://doi.org/10.1109/lawp.2020.3045988.

[7] Li M., Zhang Z., Tang M. C., et al. "Bandwidth enhancement and size reduction of a low-profile polarization-reconfigurable antenna by utilizing multiple resonances." *IEEE Transactions on Antennas and Propagation* 70.2 (2021): 1517-1522. https://doi.org/10.1109/tap.2021.3111309.

[8] Li M., Zhehao Z., Ming-Chun T. "A compact, low-profile, wideband, electrically controlled, tri-polarization-reconfigurable antenna with quadruple gap-coupled patches." *IEEE Transactions on Antennas and Propagation* 68.8 (2020): 6395-6400. https://doi.org/10.1109/tap.2020.2970073.

[9] Singh R. K., Basu A., Koul S. K. "Reconfigurable microstrip patch antenna with switchable polarization." *IETE Journal of Research* **66.5** (2020): 590-599. https://doi.org/10.1080/03772063.2018.1510346.

[10] Bharathi, A., and Ravi Shankar. R.G. "A novel dual-sense polarization reconfigurable dual-band microstrip antenna." *AEU-International Journal of Electronics and Communications*, 171(2023), 154926.

[11] Sano, M., and Makoto. H. "A linearly polarized patch antenna with a continuously reconfigurable polarization plane." *IEEE Transactions on Antennas and Propagation* 67, no. 8 (2019): 5678–5683. https://doi.org/10.1109/tap.2019.2916660.

[12] Palanisamy, S., Obaid, A. J., Thiyagarajan, P., et al. "Miniaturized stepped-impedance resonator band pass filter using folded SIR for suppression of harmonics." *Mathematical*

Modelling of Engineering Problems 11, no. 8 (2024): 1997–2004. https://doi.org/10.18280/mmep.110801.

[13] Sathishkumar, N., Satheeshkumar, P., Rajesh, N., et al. "Experimental investigations of dual functional substrate integrated waveguide antenna with enhanced directivity for 5G mobile communications." *Heliyon* (2024): e36929. ISSN 2405-8440. https://doi.org/10.1016/j.heliyon.2024.e36929.

[14] Sathishkumar, N., Palanisamy, S., Natarajan, R., et al. "Design of dual mode antenna using CMA and broadband dual-polarized antenna for 5G networks." *Scientific Reports* 14 (2024): 15553. https://doi.org/10.1038/s41598-024-66515-x.

[15] Suganya, E., Prabhu, T., Palanisamy, S., et al. "Design and performance analysis of L-slotted MIMO antenna with improved isolation using defected ground structure for S-band satellite application." *International Journal of Communication Systems* (2024): e5901. https://doi.org/10.1002/dac.5901.

[16] Alam, M., Rezaul, A., Nebras, M., et al. "A dual-band CPW-fed miniature planar antenna for S-, C-, WiMAX, WLAN, UWB, and X-band applications." *Scientific Reports* 12, no. 1 (2022): 7584. https://doi.org/10.1038/s41598-022-11679-7.

[17] Kang, L., Li, H., Tang, B., et. al., "Quad-polarization-reconfigurable antenna with a compact and switchable feed." *IEEE Antennas and Wireless Propagation Letters* 20, no. 4 (2021): 548-552. https://doi.org/10.1109/LAWP.2021.3056549.

[18] Tang, M.-C., Yang, X., Li, W., et. al., "Polarization-reconfigurable Yagi-configured electrically small antenna." *IEEE Transactions on Antennas and Propagation* 69, no. 3 (2020): 1757-1762. https://doi.org/10.1109/TAP.2020.3018554.

[19] Sam, P. J. C., Surendar, U., Ekpe, U. M., et al. "A low-profile compact EBG integrated circular monopole antenna for wearable medical application." In: Malik, P. K., Lu, J., Madhav, B. T. P., Kalkhambkar, G., and Amit, S. (eds) *Smart Antennas.* EAI/Springer Innovations in Communication and Computing. Springer, Cham, 2022. https://doi.org/10.1007/978-3-030-76636-8_23.

[20] Zhang, Y., Shu, L., Li, Y., et al. "Wideband pattern- and polarization-reconfigurable antenna based on bistable composite cylindrical shells." *IEEE Access*, vol. 8, 2020, pp. 66777-66787. https://doi.org/10.1109/ACCESS.2020.2986353.

[21] Ye, Q.-C., Li, J.-L., and Zhang, Y.-M. "A circular polarization-reconfigurable antenna with enhanced axial ratio bandwidth." *IEEE Antennas and Wireless Propagation Letters* 21, no. 6 (2022): 1248-1252. https://doi.org/10.1109/LAWP.2022.3162720.

[22] Singh, R. K., Basu, A., and Koul, S. K. "Reconfigurable microstrip patch antenna with polarization switching in three switchable frequency bands." *IEEE Access* 8 (2020): 119376-119386. https://doi.org/10.1109/ACCESS.2020.3005482.

[23] Qin, P.-Y., Guo, Y. J., and Wei, G. "A dual-band polarization reconfigurable antenna for WLAN systems." *IEEE Transactions on Antennas and Propagation* 61, no. 11 (2013): 5706-5713. https://doi.org/10.1109/TAP.2013.2279219.

[24] Mu, Y., Han, J., Xia, D., et al., "The electronically steerable parasitic patches for dual-polarization reconfigurable antenna using varactors," *The Applied Computational Electromagnetics Society Journal* (ACES), 2022, pp. 58–67. https://doi.org/10.13052/2022.aces.j.370107.

[25] Palanisamy, S., Karunanithi, S., Periyasamy, B., et al., "Hybrid CNN-GNN framework for enhanced optimization and performance analysis of frequency-selective surface antennas," *International Journal of Communication Systems*, vol. 38, 2025, p. e6105. https://doi.org/10.1002/dac.6105.

[26] Sharma, B., Indra, J., Prachi, J., et al., "The design of multi-band antenna with improved higher-order mode radiation using CMA for L5-band, L1-band, and S-band application," *Scientia Iranica*, 2023. https://doi.org/10.24200/SCI.2023.62142.7669.

[27] Palanisamy, S., Vaddiraju, A. R., Khan, A. A., et al., "Modeling of inscribed dual-band circular fractal antenna for Wi-Fi application using Descartes circle theorem," *Engineering Reports*, 2024, p. e13019. https://doi.org/10.1002/eng2.13019.

[28] Behera, K., Hirak, M., Manas, M., et al., "A compact dual-band dual-sense circular polarized wide-slot antenna for WLAN applications," *Wireless Personal Communications*, 2024, pp. 1–13. https://doi.org/10.1007/s11277-024-11357-z.

[29] Xiao, N., Wang, Y., Chen, L., et al., "Low-frequency dual-driven magneto-electric antennas with enhanced transmission efficiency and broad bandwidth," *IEEE Antennas and Wireless Propagation Letters*, vol. 22, no. 1, 2023, pp. 34–38. https://doi.org/10.1109/LAWP.2022.3201070.

[30] Yue, S., Zeng, S., Liu, L., et al., "Hybrid near-far field channel estimation for holographic MIMO communications," *IEEE Transactions on Wireless Communications*, 2024. https://doi.org/10.1109/TWC.2024.3433491.

[31] Wang, Q., Sihvola, A., Qi, J., et al., "A novel procedure to hybridize the folded transmit array and Fabry–Perot cavity with low antenna profile and flexible design frequency," *IEEE Antennas and Wireless Propagation Letters*, vol. 23, no. 8, 2024, pp. 2501–2505. https://doi.org/10.1109/LAWP.2024.3398076.

[32] Zha, S., Qu, Z., Zhang, J., et al., "A gain-reconfigurable reflector antenna with surface-mounted field-induced artificial magnetic conductor for adaptive HIRF prevention," *IEEE Transactions on Antennas and Propagation*, vol. 72, no. 9, 2024, pp. 7252–7260. https://doi.org/10.1109/TAP.2024.3434371.

[33] Wang, C., Wen, P., Huang, X., et al., "Terahertz dual-band bandpass filter based on spoof surface plasmon polaritons with wide upper stopband suppression," *Optics Express*, vol. 32, no. 13, 2024, pp. 22748–22758. https://doi.org/10.1364/OE.525298.

[34] Wen, P., Jiang, Y., Liu, F., et al., "Synthesis design of high-selectivity wideband balanced bandpass filter based on parallel coupled lines," *AEU - International Journal of Electronics and Communications*, vol. 176, 2024, p. 155159. https://doi.org/10.1016/j.aeue.2024.155159.

[35] Wen, P., Jiang, Y., Liu, F., et al., "Direct synthesis of continuously tunable wideband bandpass filtering attenuator with multiple transmission zeros," *IEEE Transactions on Circuits and Systems II: Express Briefs*, vol. 71, no. 9, 2024, pp. 4346–4350. https://doi.org/10.1109/TCSII.2024.3386034.

[36] Sathishkumar, N., Satheeshkumar, P., Osamah, I. K., et al., "Experimental investigation of a dual-mode antenna using characteristic mode analysis with enhanced directivity for GSM/5G applications," *Heliyon*, vol. 10, no. 11, 2024, p. e32217. https://doi.org/10.1016/j.heliyon.2024.e32217.

[37] Anitha, V. R., Satheeshkumar, P., Osamah, I. K., et al., "Design and analysis of SRR-based metamaterial loaded circular patch multiband antenna for satellite applications," *ICT Express*, 2024. https://doi.org/10.1016/j.icte.2024.05.002.

[38] Palanisamy, S., Rubini, S. S., Khalaf, O. I., et al., "Multi-objective hybrid split-ring resonator and electromagnetic bandgap structure-based fractal antennas using hybrid metaheuristic

framework for wireless applications," *Scientific Reports*, vol. 14, 2024, p. 3288. https://doi.org/10.1038/s41598-024-53443-z.

[39] Iqbal, J., Dhanaraj, P., Satheeshkumar, P., et al., "Analysis of electrically coupled SRR EBG structure for sub-6 GHz wireless applications," *Advances in Decision Sciences*, Asia University, Taiwan, vol. 26, no. Special, Dec. 2022, pp. 102–123.

[40] Palanisamy, S., Thangaraju, B., "Design and analysis of clover leaf-shaped fractal antenna integrated with stepped impedance resonator for wireless applications," *International Journal of Communication Systems*, vol. 35, no. 11, 2022, p. e5184. https://doi.org/10.1002/dac.5184.

[41] Suganya, E., Prabhu, T., Satheeshkumar, P., et al., "An isolation improvement for closely spaced MIMO antenna using λ/4 distance for WLAN applications," *International Journal of Antennas and Propagation*, vol. 2023, Article ID 4839134, 13 pages, 2023. https://doi.org/10.1155/2023/4839134.

[42] Palanisamy, S., Thangaraju, B., Osamah, I. K., et al., "A novel approach of design and analysis of a hexagonal fractal antenna array (HFAA) for next-generation wireless communication," *Energies*, vol. 14, no. 19, p. 6204, 2021. https://doi.org/10.3390/en14196204.

[43] Palanisamy, S., Thangaraju, B., Khalaf, O. I., et al., "Design and synthesis of multi-mode bandpass filter for wireless applications," *Electronics*, vol. 10, no. 22, p. 2853, 2021. https://doi.org/10.3390/electronics10222853.

[44] Anguraj, K., Saravanakumar, R., Praveen, K., et al., "Defected circular-cross stub copper metal printed pentaband antenna," *Advances in Materials Science and Engineering*, vol. 2022, Article ID 6009092, 10 pages, 2022. [Online]. Available: https://doi.org/10.1155/2022/6009092.

[45] Amsaveni, A., SatheeshKumar, P., Sghaier, G., et al., "Next-generation secure and reversible watermarking for medical images using hybrid Radon-Slantlet transform," *Results in Engineering*, vol. 24, p. 103008, 2024. [Online]. Available: https://doi.org/10.1016/j.rineng.2024.103008.

Technical Biography

Vinayagam K was born in 1990. He completed his Bachelor's degree in the specialization of Electronics and Communication Engineering and Master's degree in Communication Systems from Anna University, Chennai. He has six years of teaching experience and two years of industrial experience. Currently he is pursuing his research from VIT University, Vellore. His research area includes antenna design, reconfigurable and monopole antennas.

IIT-M, Chennai, and IE (I), Kolkatta, India, have bestowed the YOUNG ACHIEVER AWARD and the NPTEL MOTIVATED LEARNER AWARD, respectively, upon **Dr. SatheeshKumar Palanisamy**. Anna University, Chennai, granted him his Bachelor of Engineering (Electronics and Communication Engineering) and Master of Engineering (Communication Systems) degrees in 2009 and 2012, respectively. He qualified for the 2014 GATE examinations due to his enthusiasm for writing them. 2022 marked the completion of his doctoral studies in information and communication engineering at Anna University in Chennai. The central focus of his doctoral research was the design of multiband antennas for wireless applications. His tenure in the teaching profession spans a duration of twelve years. Antenna design, electromagnetics, RF circuit design, and wireless communication are among his areas of interest. International Association of Engineers (IAENG), Institution of Telecommunication Engineers (IETE), and International Association of Computer Science and Information Technology (IACSIT) professional memberships. At present, I am a member of the Executive Council of the IETE Coimbatore Centre. Concerning signal processing and communication systems, he has presented his work at four national conferences and in 45 articles in international journals and conferences. He serves as an international journal reviewer. Presently, he is an employee of the 5G and 6G Innovation Centre, conducting research.

Dr. N. Sathishkumar received his B.E. degree in Electronics and Communication Engineering from Anna University, Chennai, India and M.E. degree from Anna University, Chennai, India. Currently he is working as an Assistant Professor in KPR Institute of Engineering and Technology, Coimbatore, India. His current research interests include Wireless Communication, Antenna and Wave Propagation. He is a Professional member of ISTE.

Dr. Rajesh Natarajan obtained his Bachelor's degree in Electronics & Communications engineering, Master's degree (Communication Systems) and PhD from Anna University, Chennai. He has 2 years of industrial experience and 7 years of teaching experience in reputed private institutions. His research interest includes the design and analysis of UWB antennas, Frequency Selective Surfaces & Planar transmission lines. He has published 13 journal articles in reputed journals and 15 conference publications. Currently he is working as Assistant Professor (Senior) in School of Electronics Engineering, Vellore Institute of Technology, Vellore.

AARTHI GUNASEKAR received her Bachelor's degree in electronics and communication engineering from Madras University, and the M.Tech. degree in communication engineering and the Ph.D. degree from the Vellore Institute of Technology, Vellore, India. She has four years of industrial experience and 15 years of teaching experience. Her research interests include wireless optical communication (FSO and VLC),Antennas, 5G, IOT and Machine learning. She is currently an Associate Professor with the School of Electronics Engineering, Vellore Institute of Technology, Vellore, India.

List of Figure Captions:

Fig. 1 A chart illustrating the antenna design process

Fig.2. (a) Top view of the antenna geometry, (b) Bottom view of the antenna geometry in the schematic of the dual-mode antenna.

Fig.3. E field distribution of the designed antenna at 5.2 GHz (a) 0^0 (b) 180^0 (c) 270^0 (d) 360^0

Fig. 4. RLC (lumped equivalent) model of PIN diodes[33] (a) ON Condition (b) OFF Condition

Fig. 5. Circuit diagram for DC biasing

Fig.6. (a) VNA setup for antenna characterization, (b) Anechoic chamber setup, (c) Front view of the fabricated DRL antenna, (d) Back view of the fabricated DRL antenna.

Fig . 7. S-Parameter (S_{11}) Characteristics of the Proposed Antenna

(a) Variations with respect to evolutionary Steps

(b) Variations with respect to Mode 1 and Mode 2

Fig. 8. Axial Ratio for Various Slot Widths (S1 = 0.1 mm, 0.2 mm, and 0.3 mm)

Fig.9. Gain and Efficiency Parametric Analysis (Measured vs. Simulated)

Fig. 10. 2D Radiation Pattern for Observing the parametric Characteristics of the Antenna (a) 5.2 GHz (b) 3.8 GHz

List of Table Captions:

Table 1. Geometrical dimensions of the proposed antenna (in mm)

Table 2. Parametric Analysis of Antenna under Various Operating Conditions of Diode

Table 3. Comparative Analysis of the Proposed Antenna with a Relevant Antenna in Observing Parametric Characteristics

Appendices

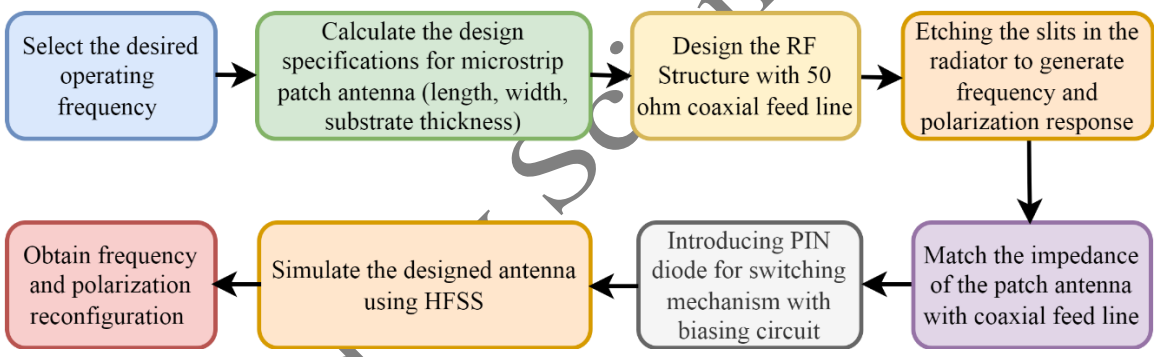

Fig. 1

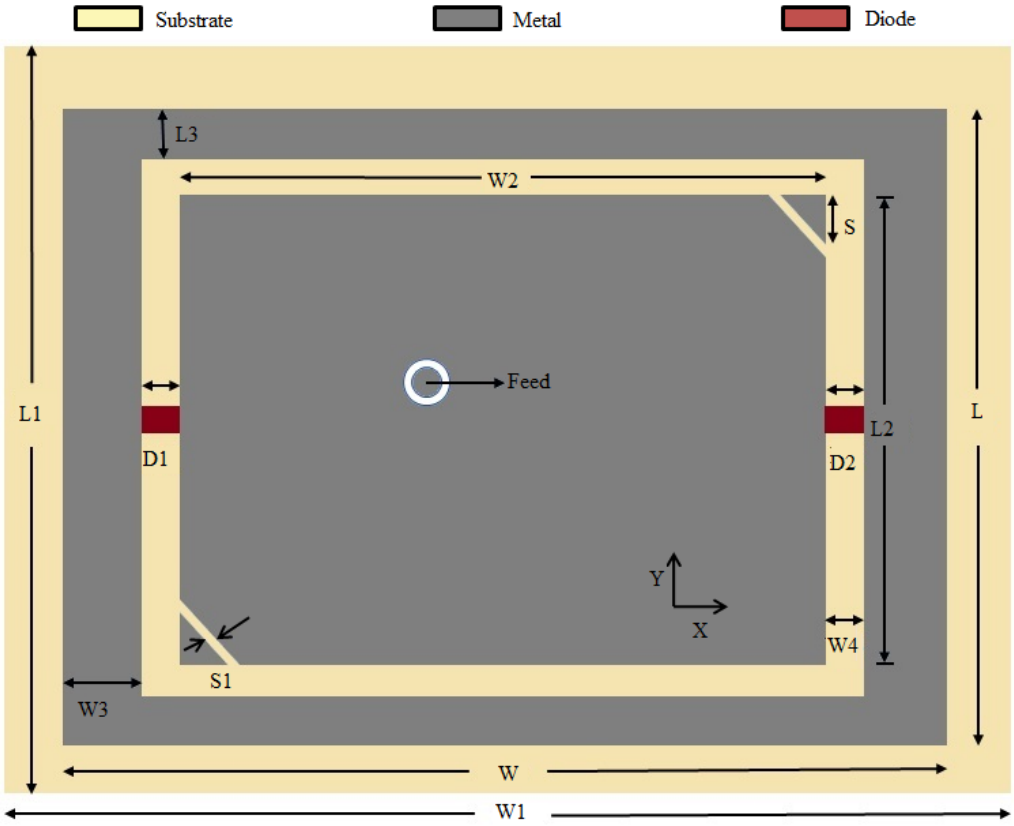
Substrate
Metal
Diode
L3
W2
S
Feed
L1
D1
D2
L2
L
Y
X
W4
S1
W3
W
W1

Fig.2. (a)

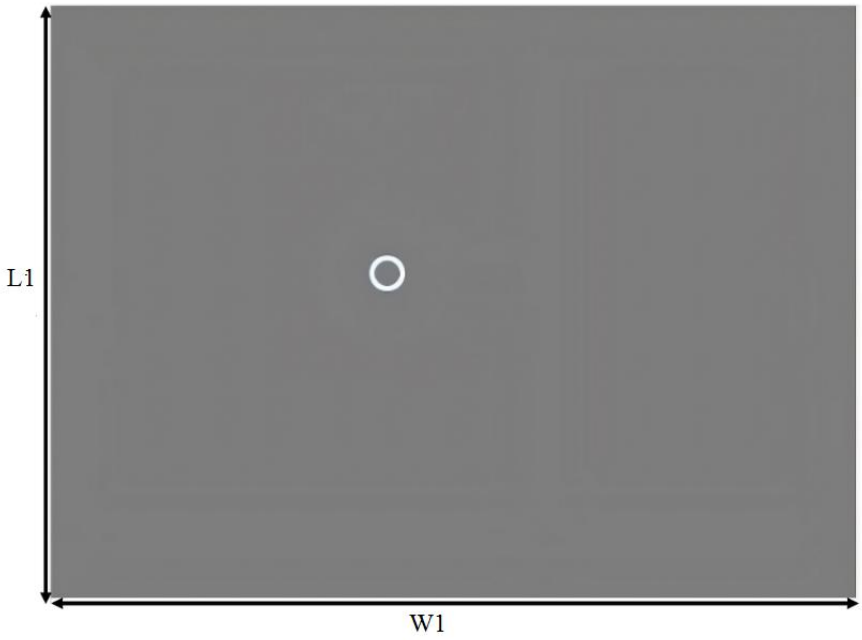
L1
W1

Fig.2. (b)

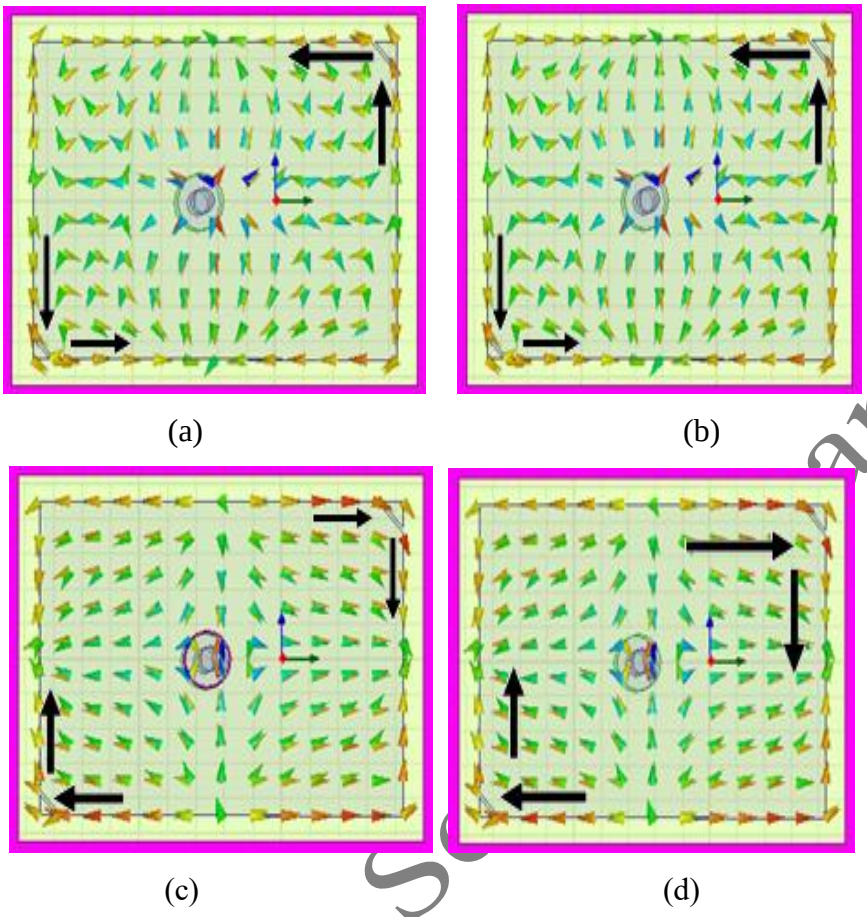

Fig.3.

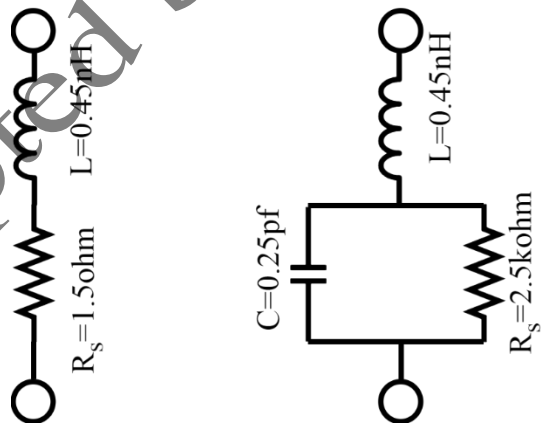

(a) **(b)**

Fig. 4.

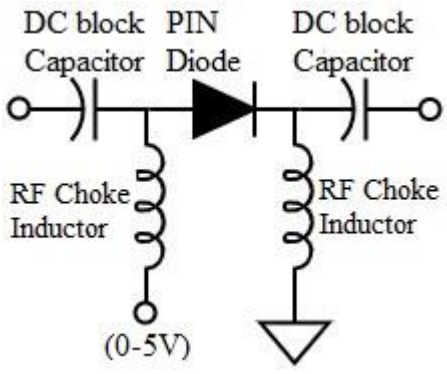

Fig. 5. Circuit diagram for DC biasing

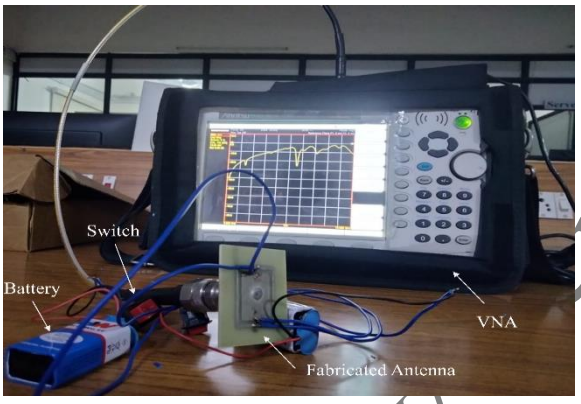

(a)

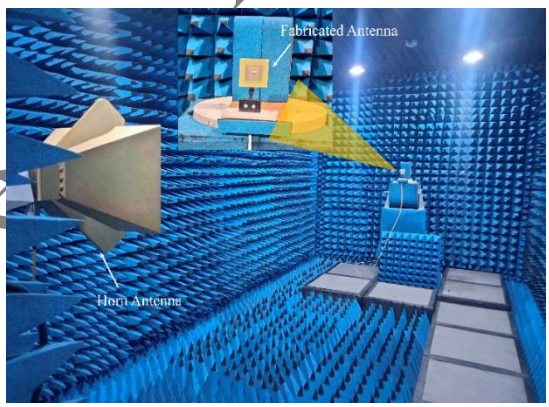

(b)

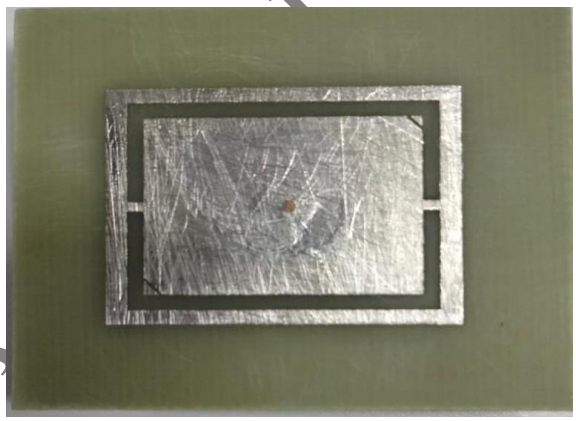

(c)

(d)

Fig.6.

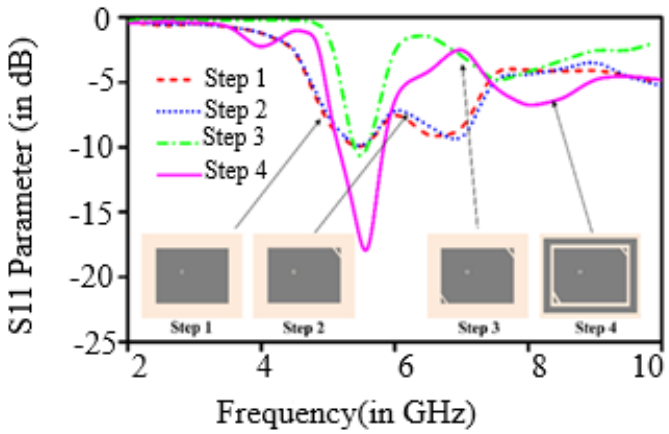

(a)

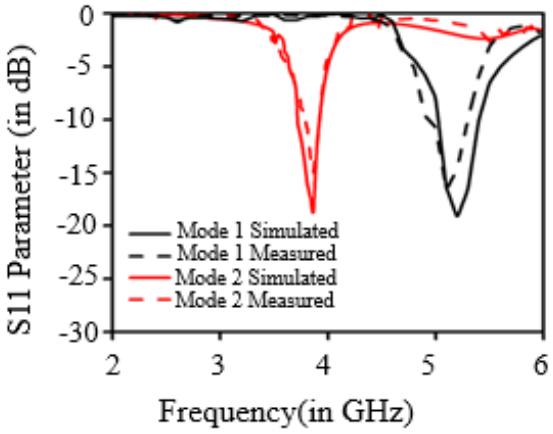

(b)

Fig . 7

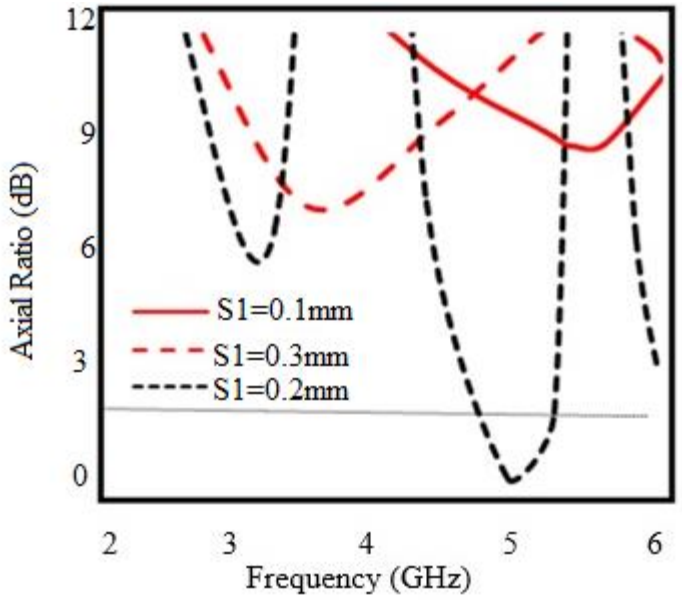
Axial Ratio (dB)
12
9
6
3
0
2
3
4
5
6
Frequency (GHz)
S1=0.1mm
S1=0.3mm
S1=0.2mm

Fig. 8.

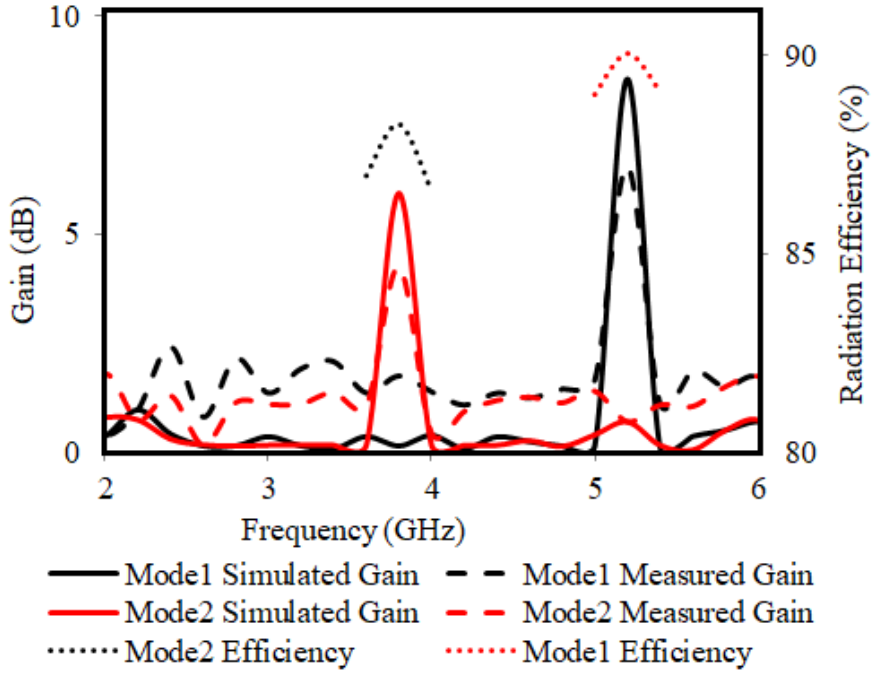
Gain (dB)
10
5
0
Radiation Efficiency (%)
90
85
80
2
3
4
5
6
Frequency (GHz)
Mode1 Simulated Gain
Mode1 Measured Gain
Mode2 Simulated Gain
Mode2 Measured Gain
Mode2 Efficiency
Mode1 Efficiency

Fig.9.

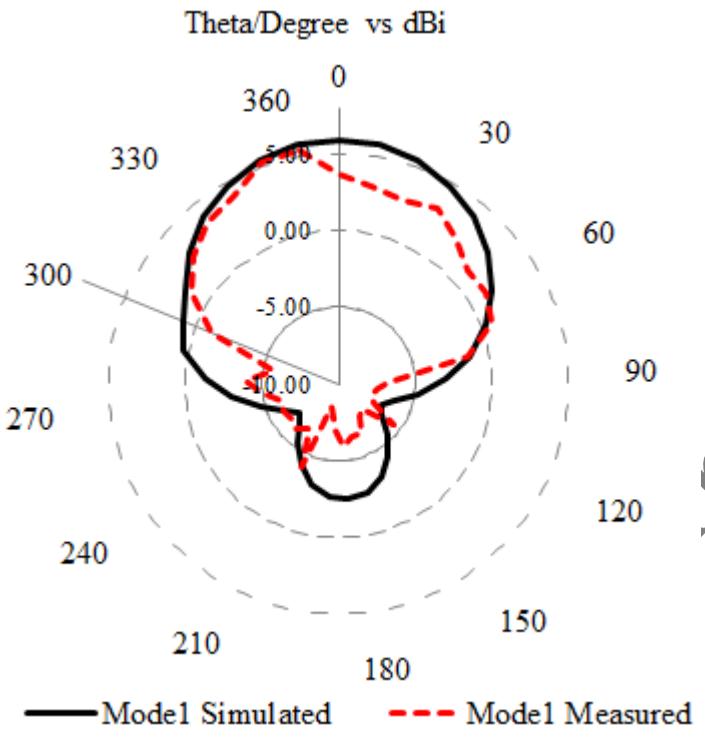

(a)

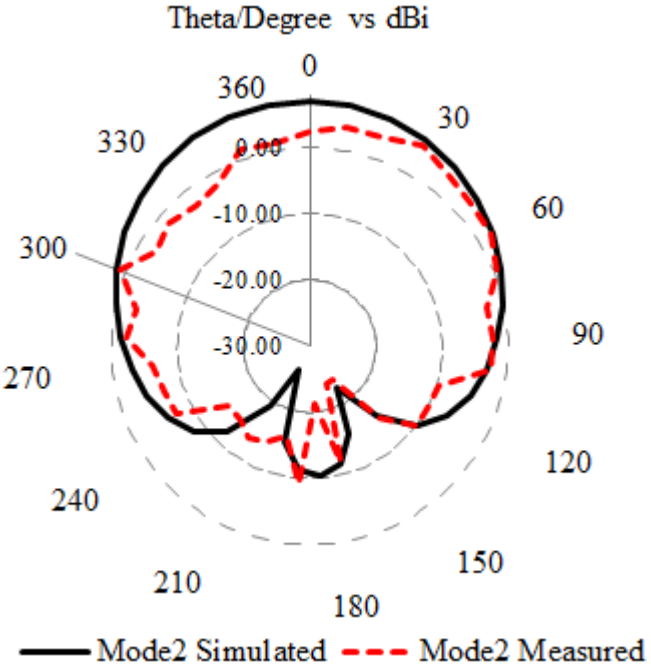

(b)

Fig. 10.

Table 1.

L	L1	L2	L3	W	W1
25.5	40	18	1.5	28.5	50
W2	**W3**	**W4**	**S**	**S1**	
24	2	1	1	0.2	

Table 2.

Diode Mode	Simulated parameters			Measured parameters		
	Modes of Operation (GHz)	S_{11} (dB)	VSWR	Modes of Operation (GHz)	S_{11} (dB)	VSWR
D1-ON D2-ON	3.8	−20	1.09	3.8	−16	1.15
D1-OFF D2-OFF	5.2	−21	1.12	5.2	−18	1.19

Table 3.

S.No	Antenna Size (in terms of λ_0)	Operating Frequency (GHz)	Polarization states	Gain (dBi)	Axial Ratio (%)	Bandwidth (%)

[7]	0.40 x 0.51	1.97-2.72	3	8	31.5	29.8
[11]	1.21 x 1.21	5.2	2	5.9	22	61
[18]	1.96 x 1.07	2.3-3	2	7.2	26.4	37
[20]	0.87 x 0.87	5.1-5.2	3	7.5-4	24-35	64
[21]	0.80 x 0.80	2.4-5.8	2	6.4-7	09-30	36-43
This Work	**0.63 x 0.50**	**5.23, 3.86**	**2**	**8.56, 5.96**	**31.10**	**78.39**